


Optimized modeling of Ni-MH batteries primarily based on Taguchi approach and evaluation of used Ni-MH batteries

Hani MUHSEN* , Ahmad AL-MUHTADY 

Department of Mechatronics and Mechanical Engineering, Faculty of Applied Technical Science,
German Jordanian University, Amman, Jordan

Received: 14.04.2018

Accepted/Published Online: 15.11.2018

Final Version: 22.01.2019

Abstract: This paper aims to generate an optimized model of the Ni-MH battery based on the Taguchi method and it further aims to evaluate used Ni-MH batteries that served in hybrid electric vehicles and electric vehicles. The status of twelve used Ni-MH batteries is studied to determine their usefulness after their life cycle in automotive applications. The status of used batteries is evaluated by investigating their state of charge, remaining useful life, and degradation in performance. Accordingly, the tested batteries are classified into four categories and they are proposed to serve in different applications. The novelty of the work lies in modeling used Ni-MH hybrid batteries by extracting a model that can define and calculate the battery voltage during the discharging phase, and it can study the influence of design parameters under certain conditions regardless of whether the battery is brand-new or used. Therefore, a second-order model is used to represent the used battery where an explicit mathematical formula expresses the discharge voltage of the new Ni-MH battery at different discharge pulse times, optimized later utilizing the Taguchi optimization method. Finally, the discharge voltage obtained using the developed model for different batteries is benchmarked against the actual measured discharge voltage by calculating the root mean square error.

Key words: Ni-MH battery, life cycle, state of charge, battery modeling, Taguchi optimization

1. Introduction

Recently, environmental awareness and adopted policies have encouraged significant shifts towards limiting CO₂ emissions and supporting nonpolluting energy sources [1]. One of the impacted sectors is the vehicle industry, which led to a growing demand for hybrid electric vehicles (HEVs) and electric vehicles (EVs). Despite the enormous benefits of HEVs and EVs, the technology still provides limited attention to the impact of the retired batteries of these vehicles after the end of their life cycles. Meanwhile, the technology of EVs and HEVs is being confronted with the lack of recycling and repurposing strategies. The benefits of retired batteries from EVs and HEVs has been addressed previously in [2] and their performance can be classified based on the observational check and the capacity measurements. This challenge steered the establishment of a few leading companies that offer reconditioning and repairing services to prolong the life of old batteries. Nonetheless, the high cost of the recycling encouraged consumers to consider the replacement option rather than the reconditioning option [3], especially with the decreasing prices of new batteries. Strategic plans for introducing cheap recycling technologies and repurposing applications must be provided to limit the undesirable impacts and to cope with the significant increase of used batteries [4]. Therefore, these automotive-application-retired batteries must be

*Correspondence: hani.mohsen@gju.edu.jo

assessed, and they must be modeled to analyze their behaviors. It is evident that there is a need to study the impact of the operation time on the model's parameters in comparison with new batteries. The modeling can help in understanding the current status of the old batteries and the possibility to recruit them in applications that require fewer capabilities or are less prone to catastrophic failure as in the automotive field. Moreover, the dynamic modeling of batteries is important for studying, designing, and simulating battery-powered electronic systems. It is also essential for representation of battery performance, performance degradation, and lifetime prediction and it is an efficient tool for power management of batteries [5–8]. In this respect, this work is purposed to test used Ni-MH hybrid batteries, to analyze their characteristics, and to generate electrical models that represent the used batteries. In the first phase, the tests will lead to determining the status of the used batteries and their remaining useful life (RUL) to repurpose them in secondary applications considering the requirements of diverse applications. The scheme of tests is valid for all the batteries, which must share the same type but differ in age and performance. In this context, it is worth studying the main parameters that represent the state of the battery. These parameters are the state of the charge (SOC), relative energy capacity (REC), and performance degradation of the battery after its lifetime in automotive applications. The next phase aims to propose an optimal model for used Ni-MH batteries. The optimal modeling process aims at estimating the model parameters through prediction of their ranges in the first place. The measurements of a brand-new Ni-MH battery (mainly the discharge voltage with constant current load) and an explicit mathematical model proposed in [9] are utilized to find the minimum and maximum possible values of the unknown model parameters. The previous step is essential to define the optimization intervals, which are necessary for the optimization process to accurately determine the optimal values of each model parameter. Taguchi's method [10] is selected to perform the optimization process due to its ability to solve complicated problems with a small number of experiments in the optimization process. Taguchi's method is easy to implement and converges to the desired objective quickly. The optimal values have been used to model the used batteries with minimum RMSE, which represents the error between the measured discharge voltage and the estimated discharge voltage of the optimized model.

2. Assessment and applications

2.1. Battery selection

Local automotive shops were surveyed to identify the current market regarding used batteries and storage and disposal methods. During this step, general background information about the batteries used in hybrid electric or hybrid vehicles was collected, where various batteries types and their manufacturer's specifications were identified, studied, and compared. Standard operating conditions were identified in this stage as well. It was found that most of the used batteries belong to the Ni-MH type, which was the reason to select this type in our study. Table 1 summarizes the manufacturer's specifications for this type of batteries. An IMAX B6 charger/discharger was used for the charging and discharging processes. The applied tests in this work are classified as nondestructive tests since destructive tests are not useful due to the divergence of test results. This divergence returns to the dependency on the batteries' origins, ages, usage, and operation conditions, unlike new batteries, which share the same test conditions. In all, twelve Ni-MH batteries have been selected to investigate their performance and sustainability in multiple applications.

2.2. Assessment parameters

The performance of the used Ni-MH batteries is determined by considering the practical parameters. One of these critical parameters is the state of health (SOH), which provides a degree of the performance degradation

Table 1. Typical Ni-MH battery cell characteristics from [11] and [12].

Parameter	Typical value
Nominal voltage	1.2 V
Open circuit voltage	1.25–1.35
Typical end voltage	1.0 V
Charge time	1.5–3 h
Charge current	0.1–1 C
Charge efficiency	70%–90%
Charge voltage	1.4–1.6 V
Temperature range	5°–40°

and can be used to estimate the remaining useful life of the examined battery [13]. The SOH is defined as the ratio of the maximum charge capacity of the old battery relative to the maximum charge capacity of the new battery.

$$SOH\% = \frac{\text{max. A.h (used battery)}}{\text{max. A.h (new battery)}} \times 100\%. \quad (1)$$

In this paper, the SOH parameter will be replaced by the relative energy capacity (REC), explained below, which contributes to a precise estimation of the SOH in the case of used batteries. The next investigated parameter is the state of charge (SOC), which depends on the operating conditions of the battery, the load current, and the temperature. Therefore, it is crucial to estimate this parameter for used batteries. The SOC plays a role in determining the safe operation of the qualified batteries, and it is defined as the residual capacity of the used battery relative to the rated capacity given by the manufacturer. The remaining capacity represents the charging or discharging capacities relative to the rated charging or discharging capacity of the new battery.

$$SOC\% = \frac{\text{remaining capacity}}{\text{rated capacity}} \times 100\%. \quad (2)$$

The SOC of the battery ranges from 0% for an empty battery to 100% for a fully charged battery, and it is extracted from the positive discharging current:

$$SOC(t) = \left(1 - \frac{1}{\text{A.h capacity}} \int_0^t i(\tau) d\tau\right) \times 100\%. \quad (3)$$

Another mathematical representation to determine the SOC is given by a differential equation [13]. Again, this relation is relevant when the discharge current is positive.

$$\frac{d(SOC(t))}{dt} = -100 \frac{i(t)}{\text{A.h capacity}}, \quad i(t) \geq 0. \quad (4)$$

It is also necessary to estimate the remaining useful life (RUL) of the used batteries by determining the number of cycles that the used battery can sustain before it fails in achieving the demanded performance [14]. Hence, a degradation test must be performed on the investigated batteries. The degradation performance is addressed in the next section. The final investigated parameter is the relative energy capacity (REC), which is used to determine the state of the battery and the remaining useful life by comparing the maximum energy that the

used battery can sustain (after charging at predetermined conditions) to the one held by a brand-new one, and it is expressed as:

$$REC\% = \frac{\text{used battery energy}}{\text{new battery energy}} \times 100\%. \quad (5)$$

To summarize, the proposed approach first considers the evaluation of the REC, SOC, and performance degradation. Then the evaluation results enable the classification of the twelve batteries, which is critical to prove their serviceability.

2.3. Ni-MH battery performance

The carried out test involves three cycles of charging and discharging, such that each iteration aims at showing the new RUL. A testing scheme for the batteries is examined after that. This scheme, which comprises several charging and discharging cycles under controlled conditions, is used to benchmark the used batteries against new batteries. The status of the investigated used batteries is then determined. The efficiency of the approach will propel change in the circuitry throughput to achieve better results through the communication between the IMAX B6 and the programmed Arduino. The Arduino was programmed to save data every second by gathering the feedback data from the voltage, current, and temperature sensors. Ni-MH batteries have specific charging characteristics (typically used), as summarized in Table 1. The IMAX B6 is supplied by a DC power supply in a range of 11 V up to 18 V [15], which in turn delivers the DC current to the tested battery. The applied voltage to the battery will always be slightly higher than the battery voltage at any given moment to ensure the charging voltage levels. The maximum permissible voltage ranges from 1.4 V to 1.6 V per cell. In the studied case, the Ni-MH module consists of six cells; therefore, the voltage of a battery module will range between 8.4 V and 9.6 V. Hence, the maximum voltage that the battery can incur is 9.6 V charged with a current of 3.25–6.5 A, which corresponds to a charge of 0.5–1 C.

Applied voltage above 9.6 V can cause severe battery destruction, and it can lead to a battery explosion or it can release dangerous chemicals. For safe charging, the batteries have been charged maximally at 9 V, which complies with the rated voltage by the IMAX B6 manufacturer. The test was set to stop when the battery voltage reached the rated value to avoid overcharging. Furthermore, the charging process must be immediately stopped if the module temperature reaches 40 °C or increases at the rate of 1 °C per minute [11]. Consequently, the Arduino has been programmed to terminate the test automatically when one of these two hazards occurs. Undoubtedly, the charging time of Ni-MH batteries is dependent on the capacity of the battery as well as the internal resistance. In other words, the duration of charging of the battery varies between different used batteries due to their different SOH and REC. The IMAX B6 and heavily resistive loads are used separately to discharge the battery. The discharge process starts when the battery is fully charged at a rated current of 0.56 A. In the discharge phase, two conditions have been set to validate the test. First, the test must be accomplished with high depth of discharge to ensure harsh discharging conditions. Second, the minimum discharge voltage level (at which discharge is terminated) was set to 5 V in the IMAX B6 according to manufacturer specifications [15].

2.4. Assessment of used Ni-MH hybrid batteries

The results of one cycle of charging and discharging for the twelve used Ni-MH batteries after their automotive life cycle have been compared with the results of a new battery. The obtained results of the three tests are given in Table 2. The charging capacity in column 2 was calculated by integrating the current readings during

the charging part over time. Similarly, the discharging capacity in column 3 was found by integrating the discharging current over time. The instantaneous power, which is the product of the current and voltage readings at a given time instant, was integrated over time to provide the charging and discharging energies available in columns 4 and 5, respectively. Accordingly, column 6, which represents the relative energy capacity (REC) values, is calculated as in equation 5. It is undeniably true that the new battery exhibited higher capacity and higher energy storage in comparison with the used batteries during the charging and discharging, which cause degradation throughout service in automotive applications, aging the used batteries as mentioned previously. Nonetheless, some of the retired batteries were capable of receiving a charge and delivering it back during discharging that amounted to 25%–29% of the new battery’s nominal charge as in Batteries 2 and 5. The next step is to classify the tested batteries in terms of their energy relative to the energy of the new battery to show their competences. Figure 1 shows the number of batteries in each range of the relative energy capacity. According to the REC, which represents the useful energy of the tested batteries, as in Table 2, the batteries have been divided into three categories. Battery 5 and Battery 7 were swollen during the charging cycle test, which means these batteries have been exhausted and they failed in the serviceability test. The main reason behind the swelling of the batteries is the random electrochemical process that leads to increasing the size of the electrodes and the separator in the hybrid battery. It is noticed that the swelling is an indication of accelerated degradation, due to the mechanical instability and the variation of the characteristics of the electrodes. Hence, the remaining ten batteries have been classified into three categories. Category A includes the batteries with higher values of REC, Category B includes the batteries with medium range of REC, and finally Category C includes the batteries with low discharging energy and capacity. Table 3 summarizes the categorized groups and their REC ranges.

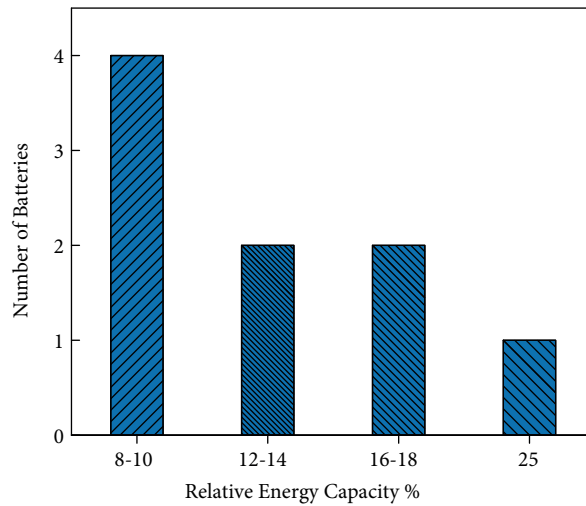


Figure 1. Relative energy capacity histogram.

Moreover, a performance degradation test was conducted on Category A batteries to ensure the capability and reliability of these batteries when it used in a secondary application. The RUL has been evaluated relying on the obtained data. The observed degradation of the battery is shown in Figure 2. The output energy of a few cycles showed a sudden increase or decrease regarding the stored energy, which causes the difference between the charging and discharging levels in the different cycles. Figure 2 shows the applied linear fitting of the energy measurements data versus the number of cycles. While exponential fitting is normally used for

Table 2. Measured capacity and energy of investigated batteries.

	Charging capacity	Discharging capacity	Charging energy	Discharging energy	REC%
New battery	6	5	51.6	37	100
Battery 1	1	1	8	6.7	18
Battery 2	1.4	1.37	11.5	9.6	25.9
Battery 3	0.5	0.5	3.7	3.3	8.8
Battery 4	1	0.8	8.1	5.2	14
Battery 5	1.75	2.1	14.5	11.4	30.9
Battery 6	0.5	0.5	4	3.3	8.8
Battery 7	0.95	1.7	7.9	9.5	25.7
Battery 8	0.52	0.48	4	3.1	8.5
Battery 9	0.84	0.9	6.6	5.9	16
Battery 10	0.62	0.5	4.8	3.3	8.9
Battery 11	0.6	0.66	4.6	4.5	12
Battery 12	0.47	0.56	3.8	4	10.7

Table 3. Capacity and energy of categorized batteries.

	Battery number	REC%
Category A	Battery 2	25.9
Category B	Battery 1	18
Category B	Battery 9	16
Category B	Battery 4	14
Category B	Battery 11	12
Category C	Battery 12	10.7
Category C	Battery 10	8.9
Category C	Battery 6	8.8
Category C	Battery 3	8.8
Category C	Battery 8	8.5

determining the RUL, in this case the battery is in the linear region as it is a retired battery working at the end of its life cycle. Therefore, the remaining life of the retired battery in cycles has been estimated assuming linear degradation to be up to 184 cycles with approximately 10% maximum error. Assuming the usefulness of the battery stops when the battery’s deliverable energy drops below 50% of its original capability when installed in the secondary application, the RUL of Battery 2 can then be calculated as 93 cycles. Accordingly, the test results showed that Category A of the retired batteries could be used once a day in a secondary application for about 3 months. Throughout the tests, Category A revealed a voltage behavior that seems identical to the new batteries except for the charging and discharging times. Category B revealed a moderate charging and discharging time and finally Category C exhibited very low REC, less charging time, and less discharging time due to its low stored energy in contrast to the other categories. In the charging phase, it should be noted that the IMAX B6 generates current pulses ranging from 0 C to 1 C and this method is known as the pulse charging method, which improves the charge efficiency, prolongs the battery life, and reduces the battery temperature. On the other hand, during the discharging phase, the current exhibited a continuous waveform as a result of discharging the stored energy by an electronic-circuit load that absorbs a constant current.

2.5. SOC, energy, and load effect

The determination of SOC change rate during discharging plays a critical role in determining the battery’s state, and the discharging approach influences it. Figure 3 shows the SOC change rate of the different battery categories where the time for the full discharge of the new battery is at least four times larger in contrast to the used ones. Therefore, it is important to observe the discharged energy and the SOC change rate under different loads. Consequently, the target batteries are loaded with one DC lamp and three DC lamps and the results are displayed in Table 4. The used lamp in the test has a nominal DC voltage of 12 V, a rated power of 21 W, and a max input current of 10 A. It has been noticed that the time of discharging using 3 DC lamps is one-fourth the discharging time using 1 DC lamp with 20% to 50% reduction in the discharging energy. The reduction of the remaining energy with increasing load current leads to the increases of conduction losses in the connection wires and the thermal energy from the DC lamps. Hence, it is essential to match the secondary applications and the retired batteries considering the load impact on the remaining discharging energy.

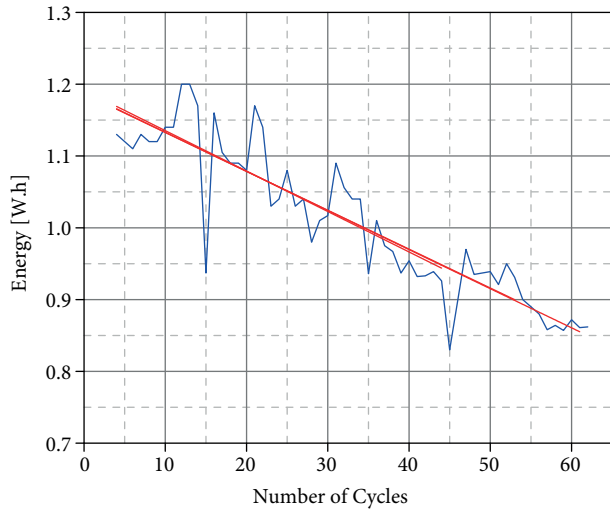


Figure 2. Degradation curve of Battery 2.

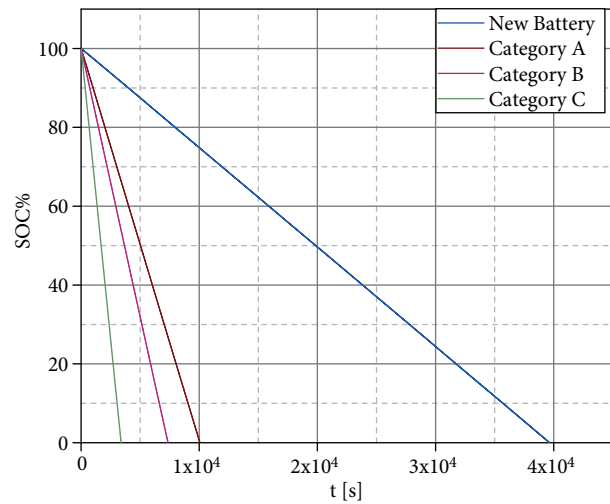


Figure 3. State of charge of the different categories.

Table 4. Discharge time and discharge energy of categorized batteries.

	1 DC lamp		3 DC lamps	
	Energy [W.h]	Time [min]	Energy [W.h]	Time [min]
New battery	39.6	250.7	28.3	61.1
Category A	9.4	62.8	7.2	16.4
Category B	6.4	45.7	5	12.2
Category C	3.9	28.1	1.7	4

3. Modeling and representation of Ni-MH hybrid batteries

Battery modeling is considered as a critical design issue to understand the battery behavior in integrated systems such as EVs and HEVs. Battery modeling can be used to estimate the SOC by connecting the external characteristics of the battery with its internal components. Furthermore, battery modeling presents a mathematical relationship between voltage, power, current, SOC, temperature, and other factors, which can

affect its performance during battery operation. Previous works addressed different battery modeling methods, which have been designed to fit different battery applications. For further details about the effectiveness of these methods, the reader may consult [16] and [17]. The battery modeling methods can be generally summarized as follows:

- Modeling based on SOC estimation [18–20].
- Empirical modeling, which includes the Shepherd model, Unnewehr universal model, and Nernst model [21–23].
- Modeling based on the equivalent circuit, which includes the Rint model, Thevenin model, PNGV model, and GNL model [24, 25].
- Electrochemical modeling [26].
- Data-driven modeling [27].

The proposed approach in this work depends on integrating the empirical modeling and the equivalent circuit modeling (mainly the general nonlinear model (GNL)). The novelty of this work lies in identifying the model parameters at different SOC based on the empirical method and the conducted measurements of the OCV, discharge current, and internal resistance. The identification of the model parameters at different SOC values will define the optimization ranges for these parameters. Afterward, the Taguchi optimization method will be used to determine the optimal values of the model parameters in order to estimate the voltage behavior of the batteries during the discharge phase. The first step to fulfill the aim of this work is to represent the Ni-MH battery by a second-order model as depicted in Figure 4. The equivalent circuit in Figure 4 consists of two pairs of parallel resistors and capacitors (R_1, C_1) , (R_2, C_2) . The two parallel branches are connected in series with a discharge resistance. All model components are supplied from a voltage source, which represents the open circuit voltage. Usually, the estimation of the model parameters $(R_1, C_1, R_2, \text{ and } C_2)$ is a complicated task. This complexity is attributed to the existence of two time constants involved in the analyzed model. The second-order model presents an advantage in that the two time constants differ significantly in magnitude, which permits dividing the test data into short-time and long-time segments. Previous efforts involved the voltage behavior of the battery in each segment to determine the model parameters [9]. The discharge resistance (R_i) is calculated by dividing the measured voltage drop on the load after 1 s over a constant discharge current of 0.5 A [13, 28].

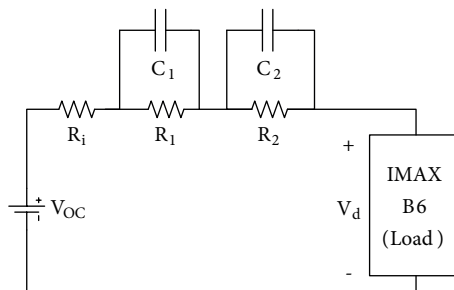


Figure 4. Second-order model of Ni-MH hybrid battery.

The discharge resistance depends on the pulse duration; hence, the duration must be accompanied by the resistance value. The discharge resistance with 1-s pulse duration is given as:

$$R_i = \frac{V_d(1) - V_d(0)}{I_d}. \quad (6)$$

The utilization of a constant current load in the discharging phase simplifies the mathematical expression of the discharge voltage, which can be given according to [9] and [19] as:

$$v'(t) = V_{oc} - I_d R_i - \sum_{m=1}^n I_d R_m (1 - e^{\frac{-t}{R_m C_m}}). \quad (7)$$

The open circuit voltage V_{oc} is assumed constant, and it represents the measured voltage of the battery before the beginning of the discharge phase. This assumption is valid if the initial voltages of the model capacitors were zero. The next step is estimating the discharge resistance and the open circuit voltage from the experimental data. Finding the values of the previous parameters leaves Eq. (7) with four unknown parameters, which represent the two pairs of R, C circuits. In pursuance of estimating the unknown parameters, the discharge voltage was collected at four equal time instants. The selected time instant is expressed as:

$$T(n) = 5n - 1, \quad n = 1, \dots, 50. \quad (8)$$

Here, T represents the pulse time used in the discharging phase. To convert the mathematical formula of the discharge voltage to a solvable form, the exponential terms can be given as:

$$d_1 = e^{\frac{-t}{R_1 C_1}}, d_2 = e^{\frac{-t}{R_2 C_2}}. \quad (9)$$

Now the discharge voltage is converted to an explicit mathematical formula, which simplifies Eq. (7) to a solvable formula as:

$$v'(t_m) = V_{oc} - R_i I_d - R_1 I_d (1 - d_1^m) - R_2 I_d (1 - d_2^m). \quad (10)$$

$$t_m = mT, \quad m = 1, 2, 3, 4. \quad (11)$$

The roots of the explicit mathematical formula represent the unknown parameters of the desired model, which is valid if the discharge voltage is collected at a specific time instant (T). First the values of d_1 and d_2 are evaluated and then x_1 and x_2 as in [9] are found by:

$$\begin{bmatrix} x_1 \\ x_2 \end{bmatrix} = \begin{bmatrix} \frac{d_2}{d_2 - d_1} & \frac{1}{d_1 - d_2} \\ \frac{d_1}{d_2 - d_1} & \frac{1}{d_2 - d_1} \end{bmatrix} \begin{bmatrix} R_o I - V(T) \\ V(T) - V(2T) \end{bmatrix}. \quad (12)$$

Next, applying the previous in the inverse of the exponential function, the values of the unknown parameters are determined as follows:

$$R_k = \frac{x_k}{I_d(1 - d_k)}, \quad C_k = \frac{-T}{R_k \ln(d_k)}, \quad k = 1, 2. \quad (13)$$

Consequently, the previous approach is repeated on the discharge voltage of the new battery at different time instants to define the optimization interval for each parameter. This step is necessary to initialize the

optimization process, which requires defining the optimization intervals of the model parameters. It is important to emphasize that the optimization intervals, which are obtained from the analysis of the new battery, will also be used for the second-hand batteries. That is, if the optimal model values are only viable for new batteries, this will render them nonuseful for evaluating and modeling automotive-retired batteries. The next step after selecting the time instants and finding the unknown parameters is calculating the RMSE by considering the measured discharge voltage and the calculated voltage based on the analytical model. The entire process to determine the ranges of the unknown parameters is summarized in an algorithm, which is depicted in Figure 5a. Figure 5b shows the values of the model parameters at different time instants and the ranges of each parameter are given in Table 5.

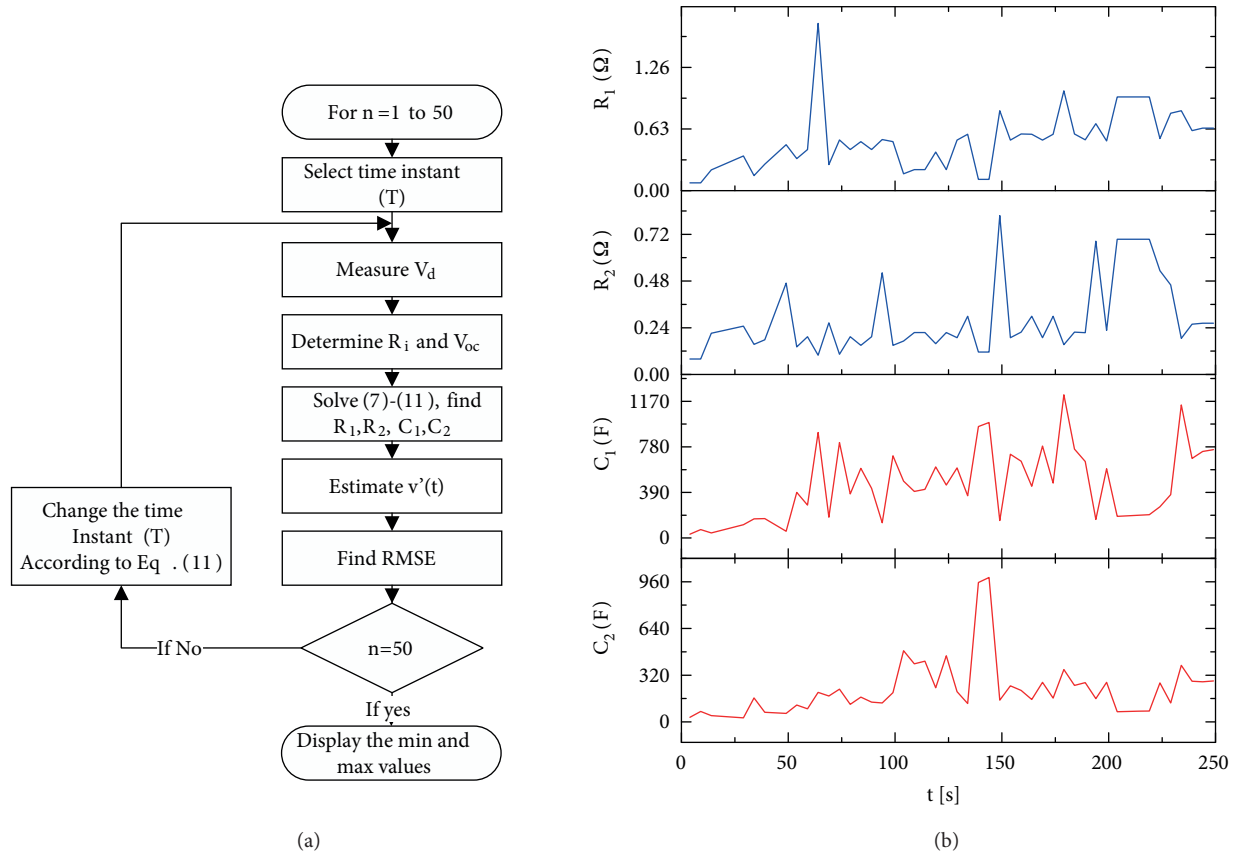


Figure 5. (a) The process of estimating the unknown parameters at different time instants and defining the optimization range, (b) estimated parameters for the second-order model versus applied time instant.

Table 5. Optimization limits extracted from the new battery discharge voltage at different discharge pulse time.

	$R_1(\Omega)$	$R_2(\Omega)$	$C_1(F)$	$C_2(F)$	RMSE
Minimum value	0.079	0.079	32	27.9	0.1254
Maximum value	1.7	0.82	1227	989	0.0857

4. Optimized modeling of Ni-MH hybrid batteries based on Taguchi method

The Taguchi method is an optimization method, which depends on using orthogonal array experiments. This optimization method provides a much-reduced variance for the experiment with optimum settings of control

parameters; further details about the Taguchi method can be found in [10]. In this section, the Taguchi optimization method is applied to extract the optimal values of the unknown parameters. The optimization is conducted for each category of the investigated Ni-MH batteries. At first, the steps of the Taguchi method are addressed; then the optimization process is applied by using the extracted intervals for each parameter as presented in the previous section. The process will terminate when the optimal values of the model parameters are identified. The optimal values will be employed in estimating the analytical discharge voltage, and the estimated behavior of the discharge voltage will be compared with the measured discharge voltage via means of the root mean square error (RMSE). The RMSE was adopted to represent the cost function in the optimization process.

The model parameters of the investigated battery are arranged in a vector $m = [R_1, R_2, C_1, C_2]$, which will be used later in the fitness function. The voltage function $v(T)$ denotes the experimental discharge voltage, and $v'(T, m)$ denotes the estimated discharge voltage by the model. Accordingly, the fitness function is defined as the RMSE between the experimental voltage and the model voltage. The RMSE is a complicated nonlinear function of the parameters, and it usually has many local minima. The discharge voltage of the analytical model and RMSE are expressed as:

$$v'(T, m) = V_{oc} - I_d R_i - \sum_{m=1}^4 I_d R_m (1 - e^{-\frac{t}{R_m C_m}}), \quad (14)$$

$$RMSE(m) = \left(\sum_{j=0}^n \frac{(v'(T, m) - v(T))^2}{n+1} \right)^{1/2}. \quad (15)$$

The discharge resistance and the open circuit voltage were evaluated for all investigated categories. The discharge voltage was measured at a discharge current of approximately 0.5 A, and the discharge pulse time (T) is set to 4. The optimization intervals of the investigated parameters in Table 5 are used to initiate the optimization process. Table 6 summarizes the values of the discharge resistance, the average value of the discharge current, and the open circuit voltage of the investigated batteries. After determining the cost function, the next step is to determine the level difference of the first iteration (L_{D_1}) for each parameter in the parameters vector (m) as follows:

$$L_{D_1}(m_j) = \frac{\max(m_j) - \min(m_j)}{s+1}, \quad j = 1, 2, 3, 4. \quad (16)$$

Table 6. Discharge resistance, exact discharge current, and the OCV for investigated batteries.

	$R_o(\Omega)$	$I_d(A)$	$OCV(V)$
New battery	0.02	0.476	8.21
Battery 2	0.02	0.485	8.09
Battery 1	0.02	0.488	8.27
Battery 12	0.02	0.476	8.22

The selected OA contains 27 experiments ($N = 27$), five control parameters ($n = 5$), and three levels ($s = 3$) and the strength is set to two ($\tau = 2$). The fifth control parameter in the OA is not used in the studied

case since the optimization of the model is subjected to four unknown parameters. The zeros in the OA denote the first level (l_1), while the ones denote the second level (l_2) and twos denote the third level (l_3). The values of the second level in the first iteration are updated by substituting the center of the optimization interval for each parameter ($x_i(m_j)$). The values of the first level are updated by subtracting the level difference (L_{D_1}) multiplied by the reducing rate (rr) from the center point, whereas the third level is updated by adding the center point to the level difference (L_{D_1}) multiplied by the reducing rate (rr). In the next iteration ($i+1$), the optimization range must be reduced by multiplying the current level difference by the updated reducing rate (rr^i). The reducing rate (rr) can be set between 0.5 and 1 depending on the problem [10] as in Eq. (17). In this work, the reducing rate (rr) is set to 0.6 due to its appropriate performance in the optimization process.

$$L_{D_{i+1}}(m_j) = rr \cdot L_{D_i}(m_j) = rr^i \cdot L_{D_1}(m_j). \tag{17}$$

$$l_{1,i}(m_j) = \min(m_j)_i = x_i(m_j) - rr^i \cdot L_{D_1}(m_j). \tag{18}$$

$$l_{2,i}(m_j) = x_i(m_j) = \frac{\max(m_j)_i - \min(m_j)_i}{2}. \tag{19}$$

$$l_{3,i}(m_j) = \max(m_j)_i = x_i(m_j) + rr^i \cdot L_{D_1}(m_j). \tag{20}$$

Table 7. Optimal values of the model parameters and corresponding RMSE.

	$R_1(\Omega)$	$R_2(\Omega)$	$C_1(F)$	$C_2(F)$	$RMSE$
New battery	0.29	0.18	377	303	5.3×10^{-14}
Battery 2	0.49	0.17	734	732	1.9×10^{-7}
Battery 1	0.26	0.12	288	231	7.2×10^{-13}
Battery 12	0.16	0.13	268	218	4.9×10^{-13}

Afterwards, the OA elements are replaced by the level values, and the RMSE is calculated for each row using Eqs. (14) and (15). This will result in 27 RMSE values in each iteration. These values are averaged according to Eq. (21) to identify the optimal level by specifying the level for each parameter that corresponds to the minimum average RMSE.

$$\overline{RMSE}(l, j) = \frac{s}{N} \sum_{i, OA(i, j)=l} RMSE_i, \quad j = 1, 2, 3, 4. \tag{21}$$

This level is assigned as the optimal level in the next iteration, and it is used as the center of optimization interval in the next iteration. After determining the optimal level, a confirmation experiment will be performed using the optimal level for each parameter.

$$x(m_j)|_{i+1}^2 = x(m_j)|_i^{opt}. \tag{22}$$

Finally, if the termination criterion is met and the optimization process converges, the optimal values will be used to model the investigated battery. Eq. (23) below represents the termination criterion, which determines the required number of iterations to satisfy that criterion.

$$\frac{L_{D_i}(m_j)}{L_{D_1}(m_j)} \leq \text{converged value}. \tag{23}$$

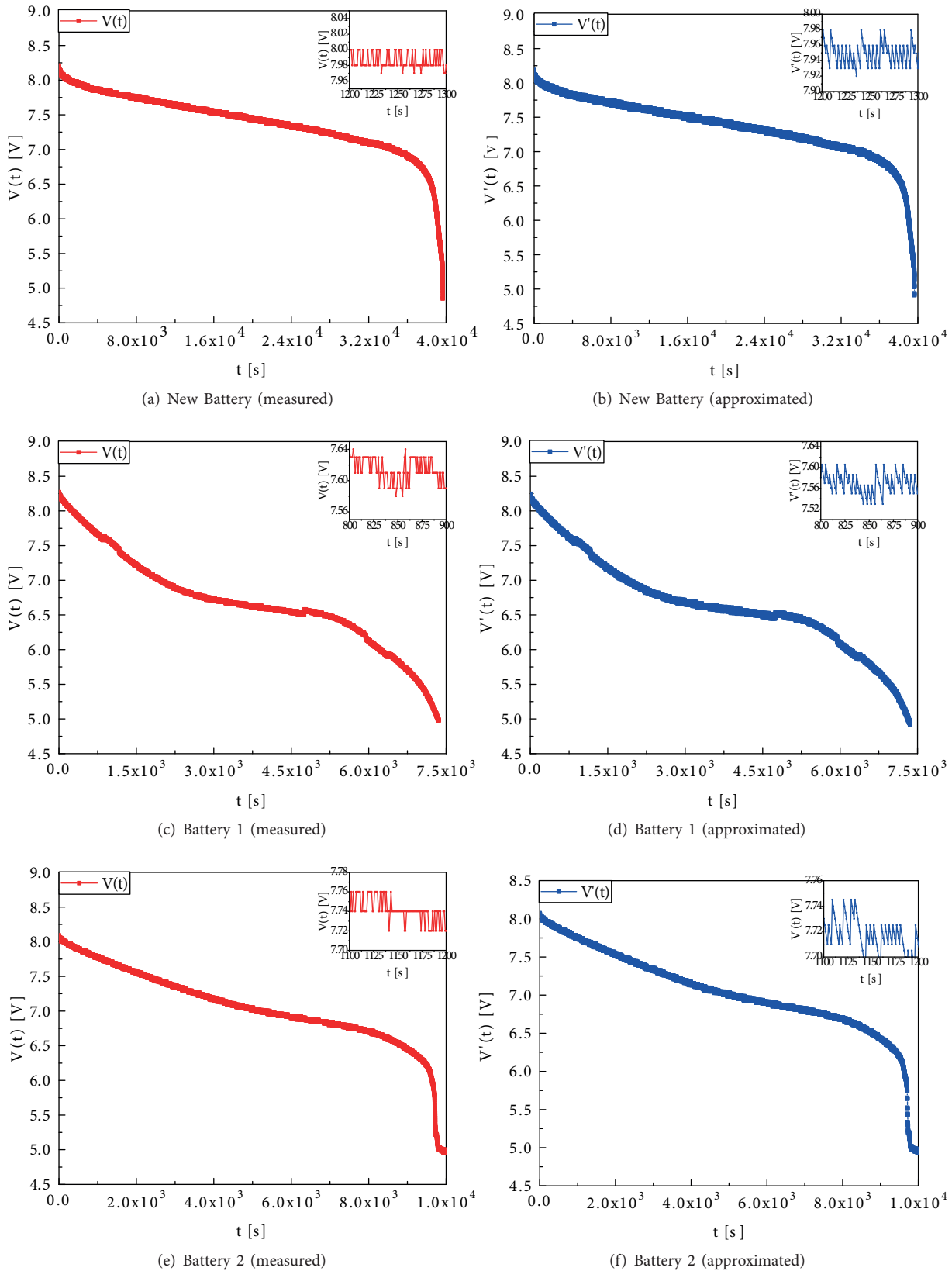


Figure 6. Comparison of the experimental discharge voltage behavior with the result of optimized second-order model of the investigated Ni-MH hybrid batteries.

Moreover, the discharge voltage of the optimized model will be compared with the measured discharge voltage to estimate the final RMSE using Eq. (15). Table 7 summarizes the optimal extracted values of the model parameters for the investigated batteries during the discharging phase under 100% SOC and at room temperature. The results show that the parameter values are approximately stable although higher discharge capacity will lead to a slight reduction in the parameters values. Hence, the proposed model is expected to predict the discharge voltage behavior of the batteries if the termination criterion was correctly set. In other words, the RMSE must be smaller than 10^{-10} to guarantee the model's accuracy and to offer high confidence in the results.

The analytical waveform of the discharge voltage of the second-order model was compared with measured discharge voltage for the investigated batteries (new battery, battery 1, and battery 2) as shown in Figure 6. The results showed the capability of the optimized model to estimate the discharge voltage behavior. The performance of the optimization process varied with the investigated batteries, which is reflected in the required number of iterations to find the global minima of the fitness function. It is worth mentioning that the number of iterations depends on the number of local minima in the RMSE function. For instance, battery 2 revealed the smallest number of iterations with 20 iterations to fulfill the optimization goals. On the other hand, battery 2 has the highest RMSE in contrast to other examined batteries. The best optimization performance was achieved for the new battery, which presented the lowest RMSE in contrast to the used Ni-MH hybrid batteries.

5. Conclusions

This work aims to evaluate used Ni-MH batteries after their retirement from service in automotive applications (EVs and HEVs), focusing on estimating their remaining useful life, performance at different loads, and applicability in different areas. Mainly, the ultimate target of the work lies in identifying a model suitable to assess these batteries' characteristics using parameters optimally found from results of one discharge cycle. First, a series of experimental charging and discharging tests on retired and new batteries are conducted. The retired batteries are then categorized based on their RECs and the rate of change of the SOC. The degradation analysis showed that batteries of Category A with 25% REC could sustain up to 184 cycles of operation, which means that they are feasibly operational for at least 3 months in secondary applications. Moreover, the load effect is investigated, whereby the energy released for higher loads was observed to be smaller. Finally, a second-order model of the Ni-MH batteries is devised. The Taguchi method was selected to obtain the optimal model parameters due to its efficiency in finding the global minimum of the fitness function (RMSE). The optimization intervals of the model parameters have been extracted by representing the discharge voltage waveform of the new Ni-MH battery by an explicit mathematical formula. The discharge voltage was collected at different pulse time instants to obtain the ranges of the model parameters. Parameters found by the Taguchi method showed competence for both new and used Ni-MH batteries, where the second-order model output matched the experimental voltages with minimum RMSE, validating the followed approach.

References

- [1] Rahman K, Hiti S. Trends in EV propulsion components and systems. *IEEE Electrification Magazine* 2017; 5: 2–3.
- [2] Liao Q, Mu M, Zhao S, Zhang L, Jiang T, Ye J, Zhou G. Performance assessment and classification of retired lithium ion battery from electric vehicles for energy storage. *Int J Hydrogen Energ* 2017; 42: 18817–18823.
- [3] Yu Y, Chen B, Huang K, Wang X, Wang D. Environmental impact assessment and end-of-life treatment policy analysis for Li-ion batteries and Ni-MH batteries. *Int J Env Res Pub He* 2014; 11: 3185–3198.

- [4] Foster M, Isely P, Standridge CR, Hasan MM. Feasibility assessment of remanufacturing, repurposing, and recycling of end of vehicle application lithium-ion batteries. *Journal of Industrial Engineering and Management* 2014; 7: 698–715.
- [5] Xia G, Cao L, Bi G. A review on battery thermal management in electric vehicle application. *J Power Sources* 2017; 367: 90–105.
- [6] Sarikurt T, Ceylan M, Balikci A. A parametric battery state of health estimation method for electric vehicle applications. *Turk J Electr Eng Co* 2017; 25: 2860–2870.
- [7] Zhang G, Chen W, Li Q. Modeling, optimization and control of a FC/battery hybrid locomotive based on ADVISOR. *Int J Hydrogen Energ* 2017; 42: 18568–18583.
- [8] Claude F, Becherif M, Ramadan HS. Experimental validation for Li-ion battery modeling using extended Kalman filters. *Int J Hydrogen Energ* 2017; 42: 25509–25517.
- [9] Hu T, Zanchi B, Zhao J. Simple analytical method for determining parameters of discharging batteries. *IEEE T Energy Conver* 2011; 26: 787–798.
- [10] Dib NI, Goudos SK, Muhsen H. Application of Taguchi's optimization method and self-adaptive differential evolution to the synthesis of linear antenna arrays. *PIERS* 2010; 102: 159-180.
- [11] Kularatna N. Rechargeable batteries and their management. *IEEE Instru Meas Mag* 2011; 14: 20-33.
- [12] Zhu WH, Zhu Y, Davis Z, Tatarchuk BJ. Energy efficiency and capacity retention of Ni–MH batteries for storage applications. *Appl Energ* 2013; 106: 307–313.
- [13] Tudoroiu N, Elefterie L, Burdescu D, Tudoroiu ER, Kec W, Dobritoiu M, Casavela VS. On-board real-time state-of-charge estimators of hybrid electric vehicles Ni-MH battery. In: 2016 8th International Conference on Information Technology and Electrical Engineering; 5–6 October 2016; Yogyakarta, Indonesia. New York, NY, USA: IEEE. pp. 1–6.
- [14] Zhu WH, Zhu Y, Tatarchuk BJ. Self-discharge characteristics and performance degradation of Ni-MH batteries for storage applications. *Int J Hydrogen Energ* 2014; 39: 19789–19798.
- [15] SkyRC Technology Co. IMAX B6 Instruction Manual. China, 2009.
- [16] Jiang J, Zhang C. *Fundamentals and Applications of Lithium-Ion Batteries in Electric Drive Vehicles*. Singapore: John Wiley and Sons, 2015.
- [17] Meng J, Luo G, Ricco M, Swierczynski M, Stroe DI, Teodorescu R. Overview of lithium-ion battery modeling methods for state-of-charge estimation in electrical vehicles. *Applied Sciences* 2018; 8: 659.
- [18] Tannahill VR, Sutanto D, Muttaqi KM, Masrur MA. Future vision for reduction of range anxiety by using an improved state of charge estimation algorithm for electric vehicle batteries implemented with low-cost microcontrollers. *IET Electrical Systems in Transportation* 2014; 5: 24–32.
- [19] Jafari M, Gauchia A, Zhang K, Gauchia L. Simulation and analysis of the effect of real-world driving styles in an EV battery performance and aging. *IEEE T Transport Electrific* 2015; 1: 391–401.
- [20] Meng J, Ricco M, Luo G, Swierczynski M, Stroe DI, Stroe AI, Teodorescu R. An overview and comparison of online implementable SOC estimation methods for lithium-ion battery. *IEEE T Ind Appl* 2018; 54: 1583–1591.
- [21] Hussein AAH, Batarseh I. An overview of generic battery models. In: 2011 IEEE Power and Energy Society General Meeting; 24–29 July 2011; Detroit, MI, USA. New York, NY, USA: IEEE. pp. 1–6.
- [22] Moore S, Eshani M. An empirically based electrosource horizon lead-acid battery model. *SAE Technical Paper* 1996; No. 960448.
- [23] Fang H, Zhao X, Wang Y, Sahinoglu Z, Wada T, Hara S, De Callafon RA. State-of-charge estimation for batteries: a multi-model approach. In: 2014 American Control Conference; 4–6 June 2014; Portland, OR, USA. New York, NY, USA: IEEE. pp. 2779–2785.
- [24] Feng J, He YL, Wang GF. Comparison study of equivalent circuit model of Li-Ion battery for electrical vehicles. *Res J Appl Sci Eng Technol* 2013; 6: 3756–3759.

- [25] Fang J, Qiu L, Li X. Comparative study of Thevenin model and GNL simplified model based on Kalman filter in SOC estimation. *Int J Adv Res Comput Eng Technol* 2017; 6: 1660–1663.
- [26] Lin C, Tang A, Xing J. Evaluation of electrochemical models based battery state-of-charge estimation approaches for electric vehicles. *Appl Energ* 2017; 207: 394–404.
- [27] Wang Y, Yang D, Zhang X, Chen Z. Probability based remaining capacity estimation using data-driven and neural network model. *J Power Sources* 2016; 315: 199–208.
- [28] Zhu WH, Zhu Y, Davis Z, Tatarchuk BJ. Energy efficiency and capacity retention of Ni–MH batteries for storage applications. *Appl Energ* 2013; 106: 307–313.